JOURNAL OF MATERIALS SCIENCE: MATERIALS IN MEDICINE 4 (1993) 431–436

Kinetics of isothermal phase transformations in a dental porcelain

M. M. BARREIRO
Facultad de Odontología, Universidad de Buenos Aires, M. T. de Alvear 2142, 1122 Buenos Aires, Argentina

E. E. VICENTE
Departamento de Materiales, Comisión Nacional de Energía Atómica, Av. del Libertador 8250, 1429 Buenos Aires, Argentina

The dissolution of leucite ($KAlSi_2O_8$) and the precipitation of sanidine ($Na_xK_{1-x}AlSi_3O_8$; $0.1 < x < 0.3$), occurring during isothermal heat treatments of a dental porcelain for porcelain-fused-to-metal restorations, was studied. The identification of phases was performed by X-ray diffraction, optical and scanning electron microscopy. An isothermal time–temperature–transformation (TTT) diagram, from 800 to 1000 °C, and for periods up to 1440 min, is proposed. No metastable cubic leucite was retained by air-quenching in any sample. No increase of leucite volume fraction was observed.

1. Introduction

Porcelain-fused-to-metal (PFM) is a widely used dental restoration in which several layers of porcelain are successively applied and fired in vacuum onto a metal framework which has been previously modelled and cast according to the anatomical conditions [1, 2]. Porcelains for PFM restorations are very different in composition and structure from the traditional or tri-axial porcelains (that is, those made by the blending and the firing of clay, quartz and potassium feldspar) [3]. Actually, the bodies of dental porcelains are partially-crystallized feldspathic glasses (Na_2O–K_2O–Al_2O_3–SiO_2 system) that consist, at room temperature, of tetragonal leucite ($K_2O \cdot Al_2O_3 \cdot 4SiO_2$ or $KAlSi_2O_6$) embedded in a matrix of glass [3–8]. Such formulations are used with a metal substrate because of their high linear thermal contraction coefficient α. Glasses obtained after complete melting and cooling of potassium–sodium feldspars ($(Na, K)_2O \cdot Al_2O_3 \cdot 6SiO_2$ or $Na_xK_{1-x}AlSi_3O_8$; $0 < x < 1$) show no great variation in value of α ($\approx 7 \times 10^{-6}\,°C^{-1}$; 20–900 °C) across the composition range [9], which is well below those of metal substrates ($\alpha \approx 14$–$16 \times 10^{-6}\,°C^{-1}$; 100–600 °C [10]). Instead, tetragonal leucite has high values ($\alpha \approx 20$–$25 \times 10^{-6}\,°C^{-1}$; 25–625 °C [11–13]). Therefore, the amount of leucite determines the average α of the porcelain. The softening behaviour and the opacity of the porcelain, are also determined by the amount of leucite [3]. The suitable quantity of leucite in the porcelain (20–30 vol % [3]) is achieved by some of the following procedures: (a) a controlled crystallization of the starting glass by means of an annealing treatment [4]; (b) the addition of powdered synthetic leucite to a powdered glass [14]; (c) the blending of two (or more) distinct glassy frits, one of them being a glass (low-fusion/low-contraction frit), and the other being a crystallized glass obtained by incongruent (peritectic) melting of potassium feldspar to leucite plus liquid, that becomes leucite plus glass upon cooling (high-fusion/high-contraction frit) [1, 2].

The firing of each dental porcelain layer usually involves a short soaking time (2–5 min), followed by a rapid-cooling (up to 600 °C min^{-1} through the glass transition temperature range [15–18]) when the prosthesis is removed from the furnace and allowed to air-cool down to room temperature. Some types of prostheses, like multi-element bridges, may require many firing cycles to achieve aesthetic-functional matching to the remaining healthy teeth. It has been reported [10, 19–21] that some porcelains have a tendency to undergo a microstructural change and a corresponding increase or decrease in α, under certain heat treatments. These changes in α can produce transient or residual tensile stresses during cooling that increase the risk of immediate or delayed failure of metal–ceramic prostheses [21]. Recently, it has been shown [22] that multiple firings and long soaking times at normal firing temperature, are capable of reducing the leucite content of dental porcelains, and of precipitating sanidine ($\alpha \approx 4$–$8 \times 10^{-6}\,°C^{-1}$; 20–700 °C [23]), which is the high-temperature solid solution (monoclinic) of potassium–sodium feldspars. Also, some fired and slow-cooled porcelains showed a tendency to increase their leucite volume fractions, with respect to rapid-cooled types [24].

It has been pointed out [3, 4, 7, 8] that typical compositions of dental porcelain bodies may be studied in the K_2O–Al_2O_3–SiO_2 ternary phase diagram [25], where liquid, leucite plus liquid, leucite plus sanidine plus liquid, sanidine plus liquid, etc., are the equilibrium phases in a descending order of temperature. These are *reconstructive* (also termed *nucleation and growth*) transformations that occur above about

0957–4530 © *1993 Chapman & Hall*

800 °C [25]. They are sluggish and irreversible. Consequently, some high-temperature structures are quenchable as metastable phases [26, 27]. Besides the above transformations, it is well known [28–32] that leucite transforms from a high-temperature structure (cubic) to a low-temperature one (tetragonal). The transformation temperature depends on the composition in the K_2O–Al_2O_3–SiO_2 system, varying over a wide range from 404 to 628 °C [30]. For natural [31] and synthetic [32] leucites this transformation has been proposed to be *displacive* (also termed *martensitic*). These transformations are immediate and reversible at the transition temperature. Metastability is precluded; that is, a high-temperature structure form cannot be preserved [26, 27]. However, some authors [4, 7, 11–13] have retained metastable cubic leucite ($\alpha \approx 11$–$13\times10^{-6}\,°C^{-1}$; 25–600 °C [11]) in some quenched leucite-containing glasses. For achieving the required average values of α, this phase is not desirable in dental porcelains for using with traditional high-contraction alloys [3], although it may not apply to titanium ($\alpha = 8.6\times10^{-6}\,°C^{-1}$; 100–500 °C [33]) and other low-contraction metal substrates.

Phase diagrams say nothing about the rate of phase transformations. A convenient form for representing the kinetics of phase transformations is by means of *isothermal and continuous time–temperature–transformation (TTT) diagrams* [26, 34, 35]. They allow prediction of the amount of each phase in samples subjected to different thermal histories. TTT diagrams are critically dependent on the initial state of the samples. Even for samples of the same composition and removed from the same equilibrium state, TTT diagrams depend on the scale of the microstructure. It is the heterogeneous nucleation of a new phase which usually takes place at interfaces, grain boundaries, etc., that strongly influence the rate of phase transformations.

The aim of this work was to study the kinetics of the reconstructive phase transformations (the precipitation of sanidine and the dissolution of leucite) of a typical dental porcelain for PFM restoration, and draw the isothermal TTT diagram. To observe the evolution of the structure towards the phase equilibria, annealing times were longer than those usually employed in dental laboratory practice. The possibility of retaining cubic leucite upon air-quenching was carefully examined.

2. Experimental procedure

The commercial dental porcelain selected for this study was *Ceramco* dentin body (Ceramco, Inc., New York 11101, USA). According to [36], it is based upon the Weinstein *et al.* patents [1, 2]. The starting powder was characterized by emission spectroscopy (semi-quantitative analysis) and X-ray diffraction (XRD) in a previous work [8]. The main constituents (> 3 wt%) found are: Si, Al, K and Na, and the minor elements (< 3 wt %) are: 1–3 wt % Ca, 0.3–1 wt % Mg, 0.3–1 wt % Zr, ≈0.3 wt % Sn, 0.1–0.3 wt % Ba, 0.1–0.3 wt % Fe, and ≈0.1 wt % Pb. Its XRD pattern showed most of the lines of tetragonal leucite and the major line of cassiterite (SnO_2).

The dried starting powders (about 1 g each) were placed into small alumina crucibles and annealed in an electric tube furnace in air. Temperatures were measured with a Pt/Pt–10 wt % Rh thermocouple. Isothermal heat treatments were carried out from 800 to 1000 °C, over 10–1440 min, followed by air-quenching (Table I). Annealing times were measured from the instant the as-received porcelain powders were placed into the thermally stabilized furnace. The annealed samples were discs of 13 mm in diameter and 4 mm in thickness. Their microstructures were examined by scanning electron microscopy (SEM), energy-dispersive spectrometry (EDS), and by reflection optical microscopy (ROM). The specimens were prepared for microscopic examination by grinding on silicon carbide paper down to 600-grit, and by mechanical polishing with diamond paste of particle size 15–7–3–$\frac{1}{4}$ μm. Then, they were chemically etched with a 1% aqueous solution of HF for 30–90 s. Finally, they were metallic coated with either aluminum (high-vacuum evaporation) for ROM, or gold (cathode sputtering) for SEM. Phases were identified by the morphology as reported previously [8], and by XRD, which will be analysed below. No quantitative analysis of the volume fractions of the phases was performed, but they were roughly estimated by ROM and SEM in many different regions of each sample.

XRD analysis was performed using Phillips PW 1400 equipment, employing graphite-monochromated CoK_α radiation at room temperature. The XRD patterns, recorded at a 2θ scan rate of $1°\ min^{-1}$ from 10 to 90°, were indexed by comparing the observed *d*-spacings with JCPDS [37] and literature data [12, 32]. The (400) and (004), (112) and (211) peaks were selected for the determination of tetragonal leucite. In cubic leucite these peaks merge into the (400) and (211) reflections, respectively [32]. The ($20\bar{1}$), (111), (130) and (131) peaks were selected for determining the sanidine crystals. In addition, the

TABLE I Heat treatments and observed crystalline phases (TL: tetragonal leucite; S: sanidine; C: cassiterite)

Temperature (°C)	Time (min)	Crystalline phases present
800	10	TL + C
800	60	TL + S + C
800	360	TL + S + C
800	1460	S + TL + C
850	60	TL + S + C
850	360	S + TL + C
850	1460	S + C
900	10	TL + C
900	60	TL + S + C
900	360	S + TL + C
900	1460	S + C
950	60	TL + S + C
950	360	TL + S + C
950	1460	TL + S + C
1000	10	TL + C
1000	1460	TL

(20$\bar{1}$) reflection was used for determining the composition of this alkali feldspar, since there is a linear relationship between the reflection values and the potassium–sodium ratios expressed in weight percentages, running from $d = 0.42301$ nm for pure potassium feldspar, to $d = 0.40334$ nm for pure sodium feldspar [38].

3. Results

ROM of polished, unetched and uncoated porcelains show pores and a very small quantity of bright, white opacifying crystals dispersed in a semi-transparent light grey matrix. The high porosity is due to heat treatments performed in air. Samples annealed at 950 and 1000 °C have nearly spherical pores (5–20 μm), while those annealed at lower temperatures exhibit more irregular pores. Only Sn was found by EDS analysis in the opacifying crystals. They are very likely to be cassiterite. Their typical size is 0.1–0.5 μm.

Progressive etching of the samples revealed features of the matrix. It is constituted of glass, and tetragonal leucite and/or sanidine, depending on the heat treatment (Figs 2–11). Table I shows the crystalline phases observed in each sample. The leucite crystals contain Si, Al and K as analysed by EDS. The sanidine crystals and the glass also contain a very small quantity of Na. The etchant heavily attacks the leucite, and slightly attacks the glass and the cassiterite. The sanidine seems to be unetched. After 30 s of etching, leucite is clearly discernible by ROM. After 60 s it is possible to resolve the sanidine. After 90 s the microstructures are distinct, although some crystals of leucite may be over-etched.

The metallic coating of the samples is necessary to eliminate overlapping of the phases and pores located on and beneath the surface, when those are examined by ROM. However, the coating increases and smooths the reflectance of all the phases and therefore it reduces the contrast between the cassiterite and the remainder of the phases. SEM of the samples reveals fine details of the leucite substructure.

XRD analysis of sanidine-containing samples showed that corresponding (20$\bar{1}$) d-spacings range between 0.4220 and 0.4185 nm. These values correspond to Na/K weight composition ratios ranging from 0.06 to 0.23, respectively [38]. Then, by a simple calculation, the formula of the observed sanidine may be written as $Na_xK_{1-x}AlSi_3O_8$; $0.1 < x < 0.3$. Fig. 1 shows the XRD patterns for the sample annealed at 900 °C for different times. Both tetragonal leucite and sanidine are present after 60 min of annealing time. In addition, leucite-containing samples, exhibit the (112) and (211) peaks in their XRD patterns at low angles (not shown in Fig. 1). It is emphasized that no cubic leucite was retained by air-quenching in any of the 16 samples.

Combining all the techniques, the microstructures for the different heat treatments can be described as follows. The specimens annealed for 10 min (Figs 2 and 3), whatever the temperatures, are rather similar to each other, except the shapes and the sizes of the pores. They have only tetragonal leucite (approxim-

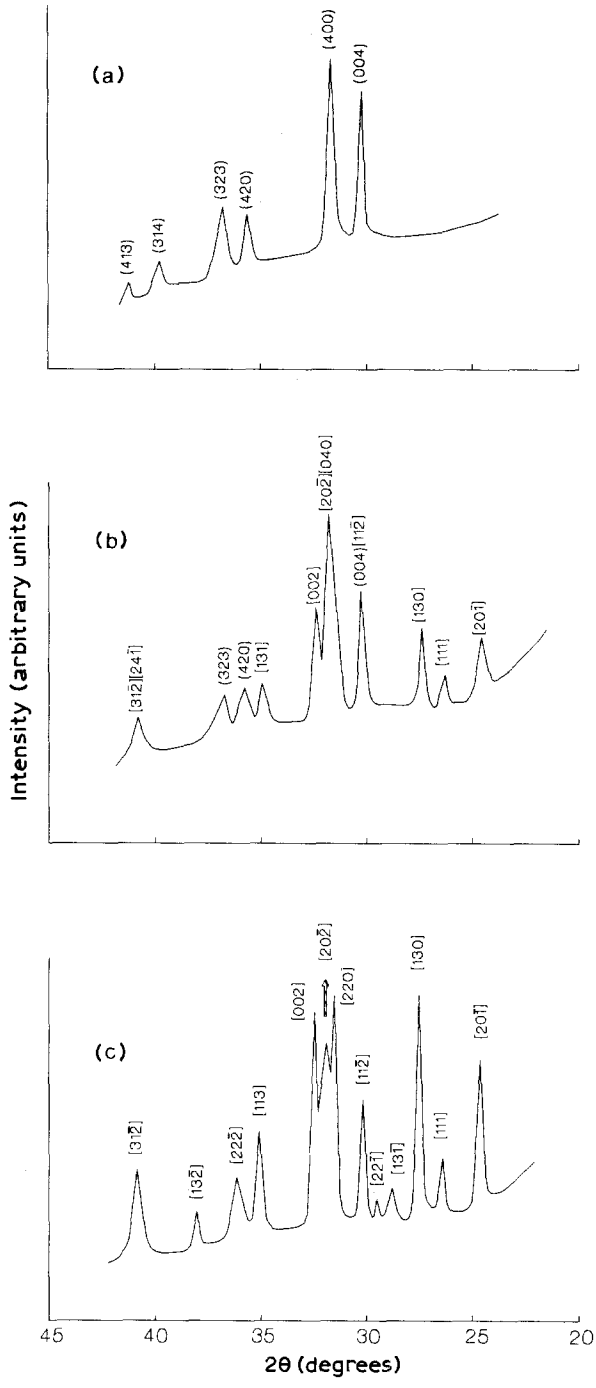

Figure 1 X-ray diffraction patterns of the samples annealed at 900 °C for: (a) 10 min; (b) 60 min; (c) 360 min. (*hkl*): tetragonal leucite; [*hkl*]: sanidine.

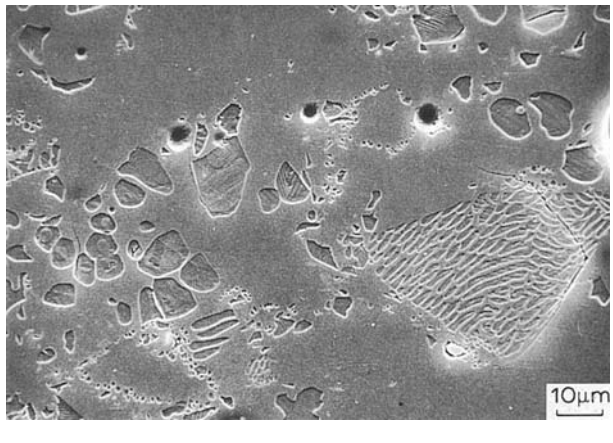

Figure 2 Porcelain annealed at 900 °C for 10 min. Tetragonal leucite crystals in a matrix of glass.

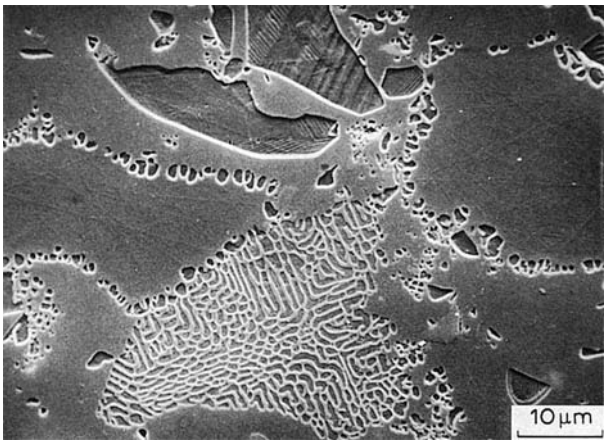

Figure 3 As in Fig. 2. Particles of different frits outlined by small leucite crystals.

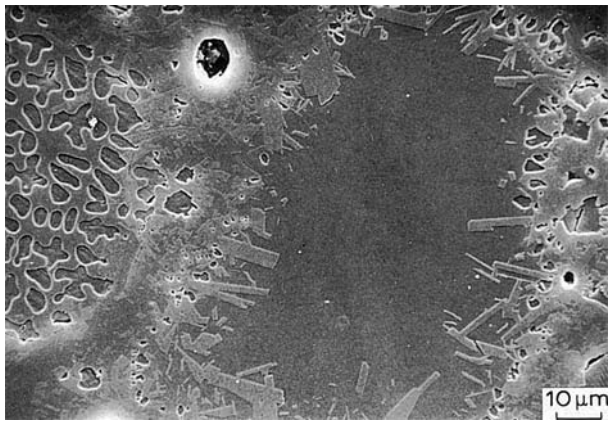

Figure 4 Porcelain annealed at 900 °C for 60 min. Crystals of tetragonal leucite (left), crystals of sanidine and glass.

ately a fourth or a fifth part of the porcelain), cassiterite and glass. Leucite crystals are inhomogeneously distributed. It is possible to distinguish irregularly-shaped zones (Fig. 3) that certainly correspond to particles of the different frits, such as those found in *Ceramco* opaque porcelain by other authors [5]. One of the zones (approximately half of the porcelain) is of an all-glass frit (e.g. component no. 2 of the Weinstein *et al.* patent [1]). They are large (20–50 µm), and they are outlined by small (about 1 µm) leucite crystals. A second zone (approximately one-third of the porcelain) is of a leucite-containing frit (e.g. component no. 1 of the Weinstein *et al.* patent [1]). It is constituted of large crystals of leucite (5–20 µm) embedded in a matrix of glass. A minor, third zone is a highly crystallized frit containing leucite (approximately one-half part of leucite in each particle), showing a fine microstructure. Each particle of this frit resembles a dendritic single crystal of leucite embracing glass in between the interdendritic spaces (0.5–1 µm). These particles seem to correspond to those which were termed 'striations' in the above quoted paper [5].

In those samples annealed for 60 min, the outline of the particles described above is hardly discernible. For longer annealing times it is not discernible at all. The amount of leucite in the sample annealed at 1000 °C for 1440 min is slightly lower than that annealed at the same temperature for 10 min. The former heat treatment also caused complete dissolution of the cassiterite crystals, so Sn was found by EDS in the glass. The samples annealed at 950, 900, 850 and 800 °C for 60 min or more, underwent precipitation of sanidine simultaneously with the dissolution of leucite and liquid phases (Figs 4–11). The kinetics of these phase transformations was found to be maximum at 900 °C. After 60 min at 900 °C the growth of sanidine is evident (Figs 4–6). After 1440 min at 900 and 850 °C leucite was almost completely dissolved, while the liquid reduced its volume fraction (Figs 7 and 8). In contrast, the samples annealed at 950 and 800 °C for 1440 min show appreciable quantities of undissolved leucite (Figs 9 and 10). The latter sample is certainly far from equilibrium. Precipitation of additional leucite in those samples annealed for more than 10 min, was not observed.

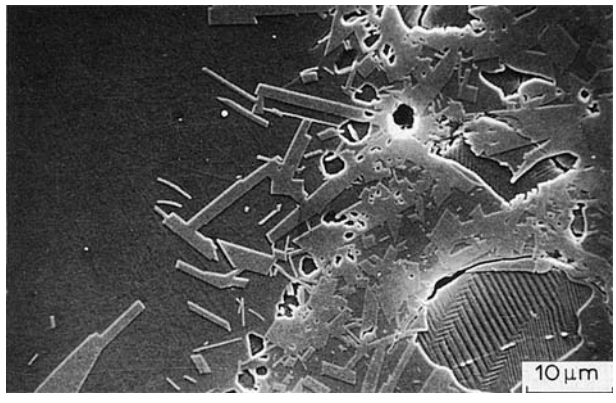

Figure 5 As in Fig. 4. Growth of sanidine crystals.

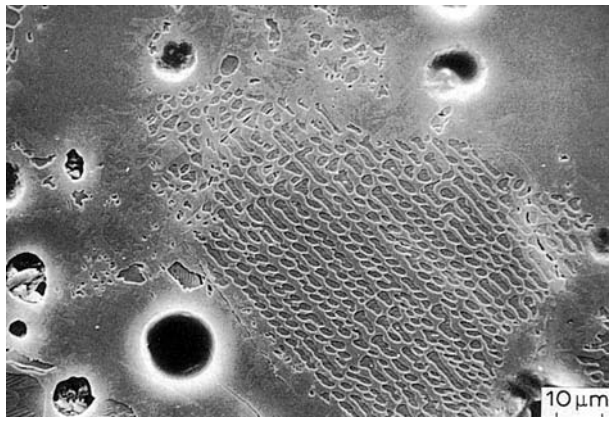

Figure 6 As in Fig. 4. Region of high content of leucite, hardly discernible sanidine and glass.

Many of the leucite crystals (especially the larger ones) have a substructure of lenticular plates internally twinned, as reported previously [8] (Fig. 5). Sanidine crystals look like untwinned plates up to about 7 µm in thickness (Fig. 8). Heterogeneous nucleation of sanidine seems to have taken place at the leucite–liquid interface, and grown towards both liquid and leucite (Figs 4, 5). As a consequence, the morphology of the remaining leucite crystals (Fig. 11) is different from that observed in the samples annealed for 10 min.

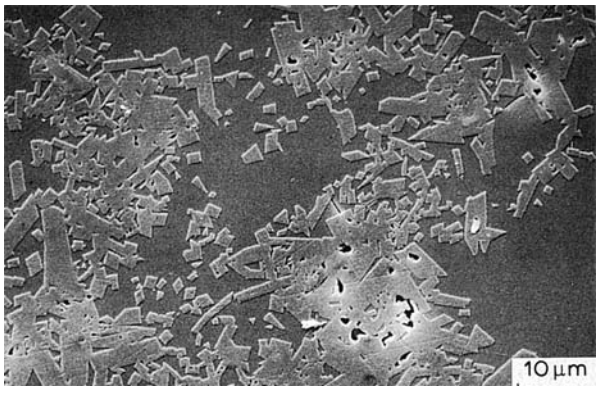

Figure 7 Porcelain annealed at 900 °C for 1440 min. Sanidine crystals and glass. Remaining leucite looks over-etched.

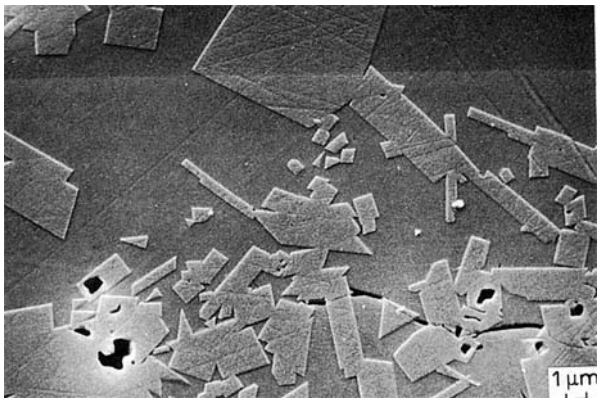

Figure 8 As in Fig. 7. Sanidine and cracked glass.

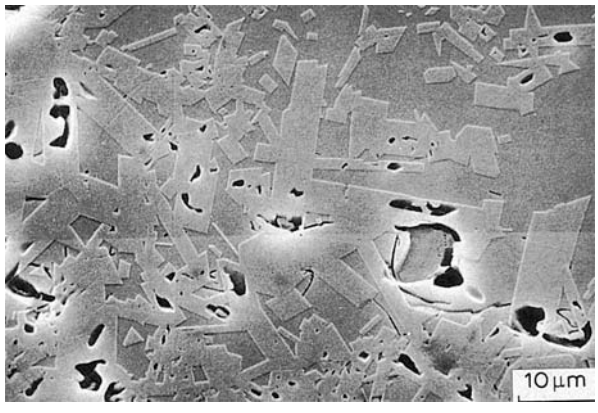

Figure 9 Porcelain annealed at 950 °C for 1440 min. Sanidine and over-etched leucite crystals in a matrix of glass.

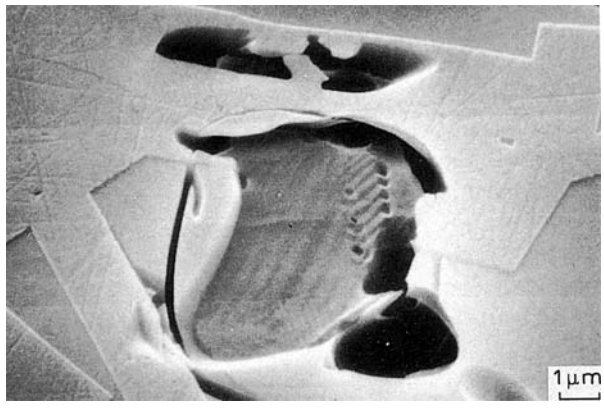

Figure 10 As in Fig. 9. Over-etched leucite surrounded by sanidine and glass.

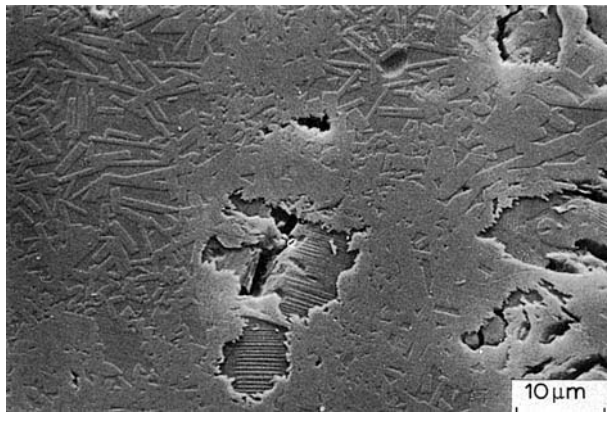

Figure 11 Porcelain annealed at 800 °C for 1440 min. Partially dissolved leucite, sanidine and glass.

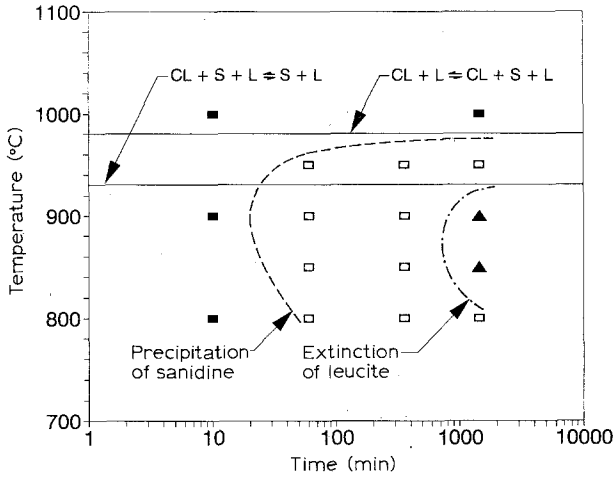

Figure 12 Proposed isothermal time–temperature–transformation (TTT) diagram of the porcelain: ■ CL + L; □ CL + S + L; ▲ S + L; – – – isotransformation curve for the precipitation of sanidine (≈5 vol % sanidine); –●– isotransformation curve for the extinction of leucite (≈5 vol % leucite). CL: cubic leucite, S: sanidine, L: liquid.

The present results are displayed in the isothermal TTT diagram of Fig. 12. The isotransformation curves for both the precipitation of sanidine (≈5 vol % sanidine) and the extinction of cubic leucite (≈5 vol % leucite) exhibit the typical *C*-shape of reconstructive transformations. The dissolution of cassiterite is not considered in the TTT diagram. The 'nose' of the *C*-curve for the precipitation of sanidine is located at approximately 900 °C and 20 min. The 'nose' of the *C*-curve for the extinction of cubic leucite is tentatively located at 850–900 °C and 700 min. The suggested temperatures of the equilibrium reactions: $CL + L \rightleftharpoons CL + S + L$ (980 °C), and $CL + S + L \rightleftharpoons S + L$ (930 °C), where CL, S and L mean cubic leucite, sanidine and liquid, respectively, are also drawn.

4. Discussion

The dissolution of leucite, as well as precipitation of sanidine, at 800–950 °C is an expected result according to the K_2O–Al_2O_3–SiO_2 ternary phase diagram [25]. The reported TTT diagram of Fig. 12 is also consistent with the results of the work in [22] done on the same porcelain, where sanidine is reported to appear after 16 firings at 970 °C, and the amount of leucite decreases with the number of firings.

At low temperatures (about 500–700 °C) sanidine should transform to other structures, but these transformations are severely limited due to the slow diffusion rates of Al and Si, requiring geological times to be achieved [39]. Hence, even in slow-cooled samples, no other crystalline structure but sanidine should be expected in dental porcelains.

Finally, the authors consider that determinations of isothermal and continuous TTT diagrams, for some currently available dental porcelains, will certainly contribute to clarification of the changes observed by many authors in thermal contraction behaviour, softening behaviour, optical properties, etc.

5. Conclusions

The isothermal TTT diagram, from 800 to 1000 °C, and for periods up to 1440 min, is proposed. The 'nose' of the *C*-curve for the precipitation of sanidine was found to be at approximately 900 °C and 20 min. The 'nose' of the *C*-curve for the extinction of cubic leucite is tentatively located at 850–900 °C and 700 min. The composition of the observed sanidine is: $Na_xK_{1-x}AlSi_3O_8$; $0.1 < x < 0.3$. No cubic leucite was retained by air-quenching in any sample. No increase of leucite volume fraction was observed in the porcelain after the heat treatments performed in this work.

Acknowledgements

The financial support for this work, given by Consejo Nacional de Investigaciones Científicas y Tecnológicas (Argentina), and by Proyecto Multinacional de Materiales OEA-CNEA, is gratefully acknowledged. The authors would also thank to Lic. S. N. Balart (CNEA) for stimulus for publication of this paper.

References

1. M. WEINSTEIN, S. KATS and A. B. WEINSTEIN, US Patent 3 052 982, September (1962).
2. M. WEINSTEIN and A. B. WEINSTEIN, US Patent 3 052 983, September (1962).
3. C. HAHN, in "Handbook of ceramics", edited by (Verlag Schmid, Freiburg, 1981) Ceramic Monograph 2.10. (See also Supplement to *Interceram* 30 (1981) No. 2).
4. C. HAHN and K. TEUCHERT, *Ceram. Forum Int./Ber. Dt. Keram. Ges.* **57** (1980) 208.
5. J. R. MACKERT, Jr., M. B. BUTTS, G. M. BEAUDREAU, C. W. FAIRHURST and R. H. BEAUCHAMP, *J. Dent. Res.* **64** (1985) 1170.
6. J. R. MACKERT, Jr., M. B. BUTTS and C. W. FAIRHURST, *Dent. Mater.* **2** (1986) 32.
7. J. R. MACKERT, Jr., M. B. BUTTS, R. MORENA and C. W. FAIRHURST, *J. Amer. Ceram. Soc.* **69** (1986) C-69.
8. M. M. BARREIRO, O. RIESGO and E. E. VICENTE, *Dent. Mater.* **5** (1989) 51.
9. P. J. VERGANO, D. C. HILL and D. R. UHLMANN, *J. Amer. Ceram. Soc.* **50** (1967) 59.
10. P. DORSCH, *Ceram. Forum Int./Ber. Dt. Keram. Ges.* **59** (1982) 159.
11. L. HERMANSSON and R. CARLSSON, in Proceedings of the Eighth International Symposium on the Reactivity of Solids, Gothenburg, 1976, edited by J. Wood, O. Lindqvist and C. Helgesson (Plenum, New York, 1977) p. 541.
12. *Idem., Trans. J. Brit. Ceram. Soc.* **77** (1978) 32.
13. M. A. ROUF, L. HERMANSSON and R. CARLSSON, *ibid.* **77** (1978) 36.
14. B. BURK and A. P. BURNETT, US Patent 4 101 330, July (1978).
15. S. W. TWIGGS, R. D. RINGLE, R. MORENA and C. W. FAIRHURST, *J. Amer. Ceram. Soc.* **68** (1985) C-58.
16. S. W. TWIGGS, D. T. HASHINGER, R. MORENA and C. W. FAIRHURST, *J. Biomed. Mater. Res.* **20** (1986) 293.
17. C. W. FAIRHURST, D. T. HASHINGER and S. W. TWIGGS, *J. Dent. Res.* **68** (1989) 1313.
18. S. W. TWIGGS, J. R. SEARLE, R. D. RINGLE and C. W. FAIRHURST, *ibid.* **68** (1989) 1316.
19. C. W. FAIRHURST, K. J. ANUSAVICE, D. T. HASHINGER, R. D. RINGLE and S. W. TWIGGS, *J. Biomed. Mater. Res.* **14** (1980) 435.
20. P. DORSCH, *Ceram. Forum Int./Ber. Dt. Keram. Ges.* **58** (1981) 157.
21. K. J. ANUSAVICE and A. E. GRAY, *Dent. Mater.* **5** (1989) 58.
22. J. R. MACKERT, Jr. and A. L. EVANS, *J. Amer. Ceram. Soc.* **74** (1991) 450.
23. A. GOLDSMITH, T. E. WATERMAN and H. J. HIRSCHHORN (eds), "Handbook of thermophysical properties of solid materials", Vol. III (McMillan, New York, 1961) p. 509.
24. J. R. MACKERT, Jr. and A. L. EVANS, *J. Dent. Res.* **70** (1991) 137.
25. J. F. SCHAIRER and N. L. BOWEN, *Amer. J. Sci.* **253** (1955) 681.
26. J. W. CHRISTIAN, "The theory of transformations in metals and alloys", 2nd edn, Part I (Pergamon, Oxford, 1975) pp. 1 and 525.
27. L. G. BERRY, B. MASON and R. V. DIETRICH, "Mineralogy: concepts, descriptions, determinations", 2nd edn (W. H. Freeman, San Francisco, 1983) p. 130.
28. D. R. PEACOR, *Z. Kristallogr.* **127** (1968) 213.
29. D. TAYLOR and C. M. B. HENDERSON, *Amer. Mineral.* **53** (1968) 1476.
30. T. HOSHIKAWA, *Yogyo-Kyokai-Shi* **84** (1976) 313.
31. F. MAZZI, E. GALLI and G. GOTTARDI, *Amer. Mineral.* **61** (1976) 108.
32. A. A. KOSORUKOV and L. G. NADAL, *Sov. Phys. Crystallogr.* **31** (1986) 148.
33. J. A. HAUTANIEMI and H. HERØ, *J. Amer. Ceram. Soc.* **74** (1991) 1449.
34. P. G. SHEWMON, "Transformations in metals" (McGraw-Hill, New York, 1969) p. 240.
35. W. D. KINGERY, H. K. BOWEN and D. R. UHLMANN, "Introduction to ceramics" (Wiley, New York, 1976) p. 320.
36. J. R. MACKERT, Jr., in "Perspectives in Dental Ceramics", Proceedings of the 4th International Symposium on Ceramics, edited by J. D. Preston (Quintessence, Chicago, 1988), p. 53.
37. Joint Committee on Powder Diffraction Standards, JCPDS Cards 15–47 (tetragonal leucite), 19–1227 (sanidine), 21–1250 (cassiterite) and 31–967 (cubic leucite).
38. A. M. MARFUNIN, "The feldspars. Phase relations, optical properties, and geological distribution" (Israel Program for Scientific Translations, Jerusalem, 1966) p. 42.
39. R. A. YUND, in "Feldspar mineralogy", edited by P. H. Ribbe (The Mineralogical Society of America, Washington, 1975) p. Y-1.

Received 19 April
and accepted 20 October 1992